Sonar Based Delineation of Oil Plume Proxies Using an AUV

Jimin Hwang
Australian Maritime College, University of Tasmania, Launceston, Australia
Email: jimin.hwang@utas.edu.au

Neil Bose
Memorial University, St. John's, Canada
Email: nbose@mun.ca

Brian Robinson
Fisheries and Oceans Canada, Dartmouth, Canada
Email: brian.robinson@dfo-mpo.gc.ca

Worakanok Thanyamanta
Faculty of Engineering and Applied Science (FEAS), Memorial University, St. John's, Canada
Email: s02wt@mun.ca

***Abstract*—Petroleum is a major pollutant that leads to climate change primarily through its combustion and the release of greenhouse gases, especially carbon dioxide. Although there is considerable interest in reducing our reliance on petroleum, to date there are limited, cost-effective alternatives to petroleum-based technologies. Petroleum leads to pollution in the oceans directly through oil spills and indirectly through the release of petroleum-based products such as plastics and tyre particles. More generally, oil spills jeopardise public health, pollute drinking water, destroy natural resources, and disrupt the economy. Oil spill response in the oceans must account for near real-time tracking of the movements of the oil to minimise damage and reduce the time for environmental recovery. However, oil patches appear on the water surface usually after the oil has been horizontally transported and vertically dispersed from an underwater source of a spill. Therefore, obtaining the 3-dimensional spatial distribution of the oil plume is critical for rapid and efficient oil spill response. Also, a non-contact method of investigation in the initial stages prior to response activities is desired in order to have as little influence on the plume as possible. In this paper, we present a set of scanning sonar tests, using a Ping360 sonar, which were conducted in Lake Barrington, Tasmania, Australia. We tested two types of relatively environmentally-friendly proxies to model patchy plumes of oil droplets. Based on the field experimental results, a method of real-time analysis of the in-situ sonar records is presented and it is shown, in simulation, how this approach can be used by an AUV to delineate an oil plume.**

***Index Terms*—autonomous underwater vehicle, marine pollutants, oil plume delineation, underwater acoustic detection, plume proxies**

I. INTRODUCTION

Tremendous efforts have been made to seek for alternative sources of clean energy in the last few decades, yet fossil fuels account for 68% of global electricity generation [1]. Burning oil produces carbon dioxide (CO_2) and other greenhouse gases that are released into the atmosphere; and they are primary contributors to climate change [2]. In fact, petroleum is closely related to global warming from its production, application and treatment. Offshore drilling operations are a source of oil leaks, oil spills and blowouts. They have also increased the chance of toxic exposure from petroleum contamination in the oceans. Moreover, a lack of technological advances in safe drilling and clean-up is ruining ocean heath.

Once oil is spilled into the ocean, it can be either mechanically recovered or ignited (in-situ burning). A review of historical oil spills has found that only 2 – 6% of a total spill is normally recovered [3]. According to records, the mechanical recovery rate of oil was only 8.3% for the Exxon Valdez [4], 9.7% for the Hebei Spirit [5] and 3.8% for the Deepwater Horizon oil spill [3]. Since clean energy will not replace our entire fossil fuel use in the near future, it is necessary to strengthen our pollutant-in-water monitoring systems, such as applying automatic detection and autonomous analysis methods.

The motivation of our work described in this paper is to develop through-the-water-column monitoring systems to track marine pollution arising from petroleum and petroleum-based products. We are developing methods to delineate discontinuous and patchy plumes that arise when oil is released into the water column and also to monitor for discrete particles, such as plastics and tyre particles [6], especially their spread over the depth of the water column. The fate of these particles and their impact on the environment, remains largely unknown. Specifically in this paper, we report on a search for an

Manuscript received September 18, 2021; revised January 10, 2022.

doi: 10.18178/ijmerr.11.4.207-214

alternative method to replace conventional fluorometer-based oil tracking approaches used to date on autonomous underwater vehicles (AUVs); so that the sensing of an oil plume can be expanded beyond that done at a series of single points.

II. Background

Fluorometers are one of the mostly commonly used underwater sensors to detect the presence of different types of oil in the marine environment [7]. They indicate the fluorometric index (FI) based upon the fluorescence of polycyclic aromatic hydrocarbons and determine the concentration of oil substances in the water column [8].

Although fluorometric sensors have been used in numerous scientific missions, the issues of their applicability in oil detection at sea has been widely discussed [9], especially in missions involved with AUVs. There are limitations in utilising fluorometers in a real ocean environment and potential issues that have been revealed during previous experiments [10].

Some fundamental disadvantages in relying on fluorometers as the primary detecting instrument for an AUV sampling mission are summarised as follows:

- An oil concentration that provides a signal lower than the minimum detection limit (MDL) of the fluorometers is not detectable.
- Ambiguity arises in the interpretation of high signals (peaks) in regions of high concentration.
- Highly sensitive fluorometers have a low signal-to-noise ratio.
- Less sensitive fluorometers rarely respond to low concentrations of oil in the water.
- Fluorometers are not capable of detecting straight-chain alkane components of hydrocarbons that may be present in the water.
- It is difficult to produce a comprehensive oil plume map through point-based measurements without making excessive physical contact with the plume.
- It is difficult to use a fluorometer to trigger the sampling of water adaptively in real time due to the fluorometer signal latency.

There are a few options that have been suggested and tested as alternatives to fluorometers by other researchers, such as multi-beam sonar [11], laser Raman spectroscopy [12] and 3D laser scanners, 3D LiDAR [13]. Although sonars have not been widely used for underwater oil detection, they have been extensively used on AUVs for underwater solid target detection. After conducting a survey for each type of these alternative sensors, an acoustic approach was decided upon for our work.

A preliminary experiment in the wave tank at the Bedford Institute of Oceanography (BIO) showed that the sonar could sense oil droplets by their acoustic intensity [10] (See Fig. 1). The outcomes from the BIO test indicated the effectiveness of two different frequencies (450kHz for a *M450* sonar and 1.35MHz for a *BV5000* sonar): the higher frequency sonar gave a stronger signal from the oil droplets. A multi-beam sonar which is a common offshore surveying tool for military, navigation and especially geological applications such as seabed mapping can be one solution. However, unlike a single beam sonar, the in-situ data is voluminous and more complex to analyse, and hence requires a lot of energy consumption and extended time for real-time data process.

A single beam sonar still does not overcome the coverage problem with point-based surveying fluorometers because it only maps a single point. Therefore, a scanning sonar (a Ping360 with frequency of 750kHz [14]) was eventually selected as the primary sensor for our AUV to detect and track an oil plume. Through sonar comparison studies, several advantages of the Ping360 compared with other types of sonar were found which included: inexpensive price, tolerance to a discontinuous shape of plume and flexibility in modification of control codes in the third-party software.

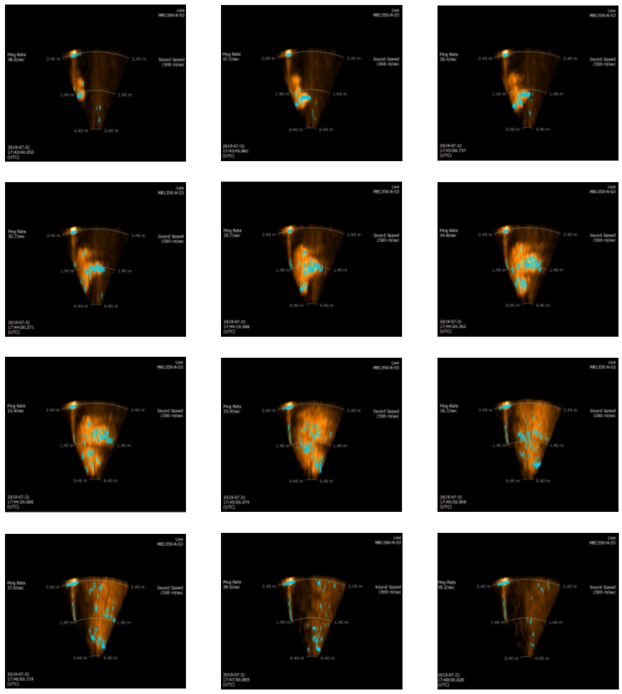

Figure 1. The BV5000 sonar images captured after the oil release.

III. Field Experiment at Lake Barrington

In order to secure a sufficient amount of data to develop a realistic sensor model and to corroborate simulation work, field tests were conducted. The main objective of these experiments was to collect acoustic measurements from a set of designated targets in a real open water environment using the Ping360 sonar.

A. *Experimental Site and Testing Conditions*

The tests were conducted in Lake Barrington, Tasmania, Australia (Latitude: -41.381700, Longitude: 146.217847) as shown in Fig. 2. A work station for dry units including a laptop, an air compressor, a power generator, cables and the sonar battery unit, was temporarily set up on the floating dock.

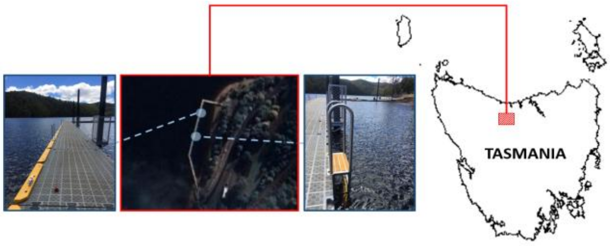

Figure 2. The floating dock (*left*); A map of Lake Barrington near Kentish Park, Tasmania, Australia (*centre*); A pool ladder allowing access to the lake (*right*).

B. Ping360 Scanning Sonar

The Ping360 is a mechanically scanning sonar that is designed primarily for localisation of target, inspecting and tracking underwater structures or objects that reflect sound waves. A narrow beam of acoustic energy is sent to the water by an acoustic transducer in the sonar head, which allows the visualisation of the surroundings around the sonar head. A sectoral image is generated as the transducer is mechanically rotated with one-degree increments as shown in Fig. 3. The sonar is capable of continuous 360-degree scanning or a sector angle can be set.

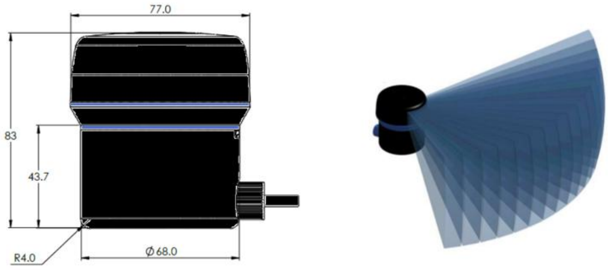

Figure 3. Ping360 Scanning sonar (*left*); Scanning coverage (*right*).

The scanning range (0.75 m – 50 m), scanning sector (0 °– 360 °) and voltage gain level (low, medium and high) can be controlled from the proprietary PingViewer software. The power was supplied through a 12-volt battery pack. The acoustic imaging was displayed as a circular sonar image in real time based on data transferred through a USB connection to the computer. The specifications of the Ping360 are given in Table I.

TABLE I. THE SPECIFICATIONS OF PING360 SCANNING SONAR

Parameter	**Value**
Supply Voltage	11 volts – 25 volts
Maximum power consumption	5 W
Communication protocols	USB, Ethernet, RS486
Cable diameter	4.5 mm
Frequency	750 kHz
Beamwidth (horizontal)	2 °
Beamwidth (vertical)	25 °
Operation range	0.75 metre – 50 metres
Range resolution	0.08% of range
Mechanical resolution	0.9 °
Scanned sector	Variable up to 360 °
Pressure rating	300 m

C. Targets (Streamers, Bubble Diffusers)

Two different targets were prepared: a plastic multi-lobed streamer with buoyancy foam attachments at the end of the streamers; and a micro-bubble generator as shown in Fig. 4. Both targets were designed and selected as potential environmentally-friendly proxies for oil droplets in open water experiments. The streamer was crafted from recycled household goods. The little foam pieces were recycled from used swimming pool floatation noodles to provide buoyancy to each streamer for effective deployment in a current.

The selected bubble generator was a Point Four™ Micro Bubble Diffuser (MBD) manufactured by Pentair, USA. This diffuser is equipped with ultra-fine pore ceramic plates which produce a cloud of fine sized bubbles in the range of 100 – 500 microns with a supplied air pressure between 1.7 to 2.4 bar.

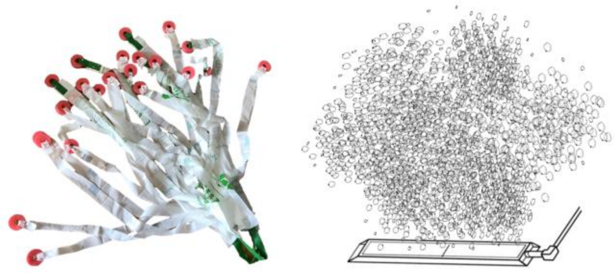

Figure 4. Plastic multi-lobed streamers (*left*); Point FourTM Micro bubble Diffuser manufactured by Pentair (*right*).

D. Equipment Configurations

The sonar was installed on an extendable pole which was attached to a ladder of the floating dock. It was lowered down to 1.5m of water depth. A waterproof cable connected the sonar to the laptop that was running the PingViewer software. The sonar was powered by a 12-volt battery pack.

Both diffuser and streamers were attached to a supporting boat. The streamers extended vertically in the water column and were kept in place by a weight mooring them to the bottom of the water and the buoyancy foam pieces at the top end of each streamer. They were lowered down to a depth of approximately 2m.

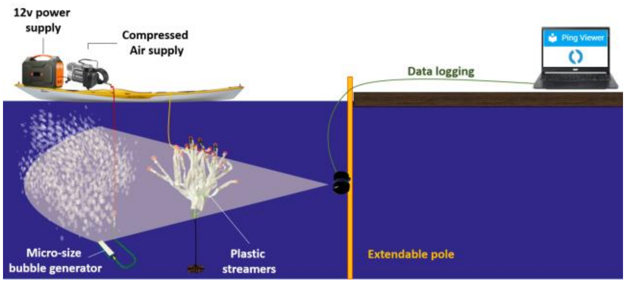

Figure 5. A schematic diagram of the test site in Lake Barrington (Not to scale).

Air was supplied to the bubble diffuser by an air compressor which was powered by a 12-volt power supply. The bubble diffuser was lowered down to a level of approximately 4m depth in the water column. During the tests, the air bubble unit and streamers were moved over a range of between 0m – 30m from the sonar.

The sonar was operated to continuously record the acoustic data for 2 hours. The lake was an uncharted area and was deeper than 7m. The equipment configuration and the setup are shown schematically in Fig. 5.

IV. FIELD EXPERIMENT

The field test results are described in this section.

A. 2D Sonar Images

Both targets were distinctively captured in the sonar records as shown in Fig. 6. With the set up used, the size of detected micro bubble plume was larger than that of the plastic streamers. They both were displayed as patches. The patch size of the streamers in the records appeared to be almost the same at different distances from the sonar within the maximum range set up to 20m, while that of the bubbles varied from a 2m to 5m spread depending on the relative distance between the sonar and the bubble generator (Fig. 7).

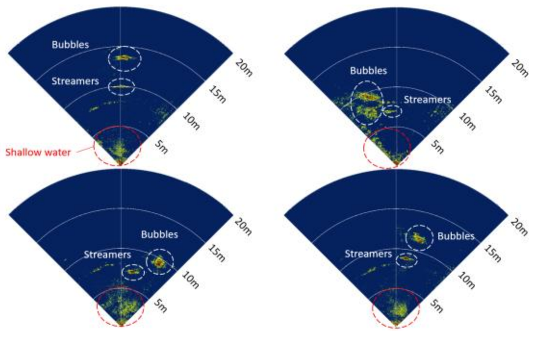

Figure 6. The Ping360 sonar images that captured the micro bubbles and the streamers. Noise reflected from the bottom of the shallower regions of the lake was also detected.

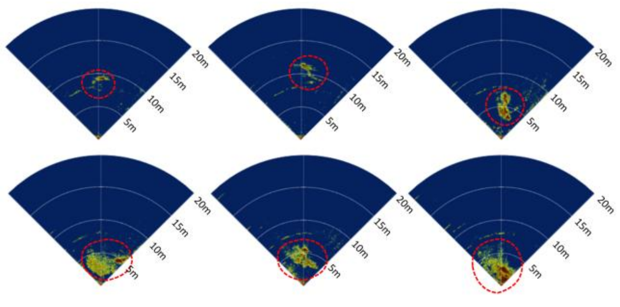

Figure 7. The Ping360 sonar images of the air bubbles during the Lake Barrington tests. The target is shown at different distances from the sonar head.

The patch size became larger when the source of the bubbles was deeper (when the diffuser was lowered). This is due to the nature of gas bubbles moving in a liquid as their volume changes due to the pressure change with depth, surface tension, and gas diffusion across the bubble surface. For example, when a bubble is injected at a depth of 1m, it will increase in volume by 10% when it rises to the surface, however, when a bubble is injected at 10m, it will double its volume as it rises to the surface. [15]. The temporal change of the gas bubble volume can be calculated using the following Equation (1) [15]:

$$\frac{d\forall_b}{dt} = -\frac{\forall_b}{P}\frac{dP}{dt} = \frac{\forall^2_b \rho_f g}{M R_g T}\frac{dz}{dt}; \quad \forall_b(0) = \forall_{ib} \tag{1}$$

where M = air mass of the bubble (calculated from the ideal gas law)
$\forall_{ib}$ = initial bubble volume
P_i = initial pressure
g = the gravitational acceleration
ρ_f = the density of fluid in which bubble moves
R_g = the gas constant for air
T = the temperature

The sonar pings were reflected from the bottom of the lake from regions of shallower water. They appeared as scattered noise in the measurements, which may confuse the search algorithm when such records are used to provide heading control to an AUV. They must be filtered out when such records are used in the process of in-situ data analysis.

The acoustic outcomes showed a high similarity in terms of shape as well as the level of measurements/signals obtained in the wave tank tests. This supports the use of microbubbles as a proxy for oil plume modelling in terms of visual (acoustic) presence in the water as well as in the measured data.

The scale of the target can potentially be upsized or downsized as occasion demands in any future field experiments. In this analysis the intensity data was constructed of 16-bit unsigned integer values, the acoustic intensity range is defined as a minimum of 0, to a maximum of 65,536.

B. 1D Measurement Analysis

The measurements from the collected data were analysed per sonar head angle. Each scanline of the data consists of its bearing angle and a series of intensity measurements divided into 600 bins, which can be expressed in a 1-dimensional line plot as in Fig. 8.

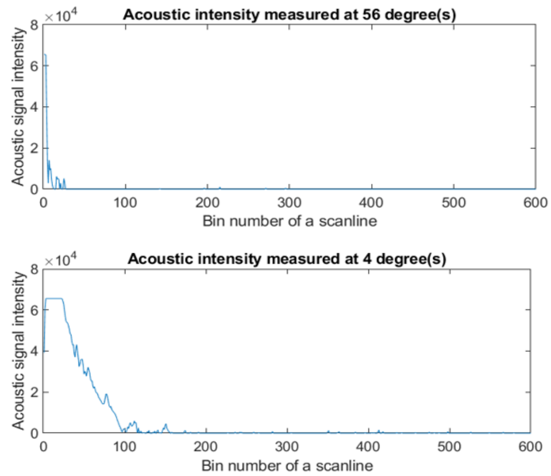

Figure 8. The plots showing 1-D acoustic measurements at a bearing angle of 56° with a range of 20m (*top*) and 4° with a range of 5m (*bottom*), respectively.

They were both instances where no target lies on the scanline, hence the default noise around the sonar head was clearly observed. This noise takes up the initial bins which varied depending on the maximum sonar range set. With a larger range, a lesser number of bins were occupied for this default noise; approximately *bin1* to *bin25* when the sonar range was 20m, and *bin1* to *bin150* when the sonar range was 5m. It is crucial to define the bins that contain this default noise around the sonar head and exclude these bins in a real-time analysis during an operation where the sonar is being used for control of an AUV.

Two further cases are compared in Fig. 9. A series of short (*bin200* – *bin250*) peaks are shown in the left plot while a longer trail of positive signature is shown in the right plot (*bin200* – *bin600*). The actual bubble patch length was approximately 1.7m and 4.0m, respectively. In the first case (the left plot), the sensed target is identifiable from a group of peaks in close proximity to one another. In the second case (the right plot), the peaks stretch to the maximum sonar range, which implies uncertainty as to whether the plume is partially or fully covered. One strategy might be designed in a way to distinguish isolated smaller patches from a larger continuous plume that extends beyond the range by observing continuity in intensity. Another strategy could be to identify the concentration of a plume through summing up the intensity measurements where the continuity condition is met; and in such a case, the range set must be taken into account as an important parameter in the analysis if sonar range is a dynamic variable.

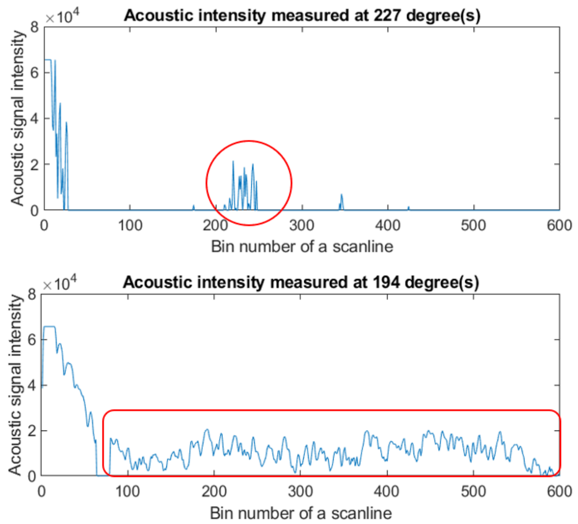

Figure 9. The plots showing a small bubble patch at a range of 20m (*top*) and a longer trail of bubbles at a range of 5m (*bottom*), respectively.

Two plots with similar conditions (the same 5m-range set and similar sized patches) are compared in Fig. 10. Both cases show multiple patches along the scanline, however different patterns were observed in their presence. The first plot contains a noisier signal in comparison with the second plot. The possible causes are twofold. Firstly, the gain value can affect these trends: there are three analogue gain setting options (low = 0, medium = 1, and high = 2) available with the Ping360. A lower gain produces a smoother trend in the sensed target in the data, while a higher gain adds minuteness by improving precision of the measurements. Therefore, a high gain setting is more preferrable in the oil plume mission of this particular application due to its sharper identification and more accurate estimation of the total oil concentration. Secondly, the size of the bubbles and/or the gap size between bubbles may lead to these two patterns, provided that the gain setting has remained constant. In this case, an algorithm for in-situ analysis must take both cases into account in order to discriminate these peaks from noise and precisely confirm each patch from other patches while tolerating discontinuity between peaks. In this particular case observed in Fig. 10, the different patterns were caused by a different gain setting: the first plot with a high gain and the second plot with a lower gain.

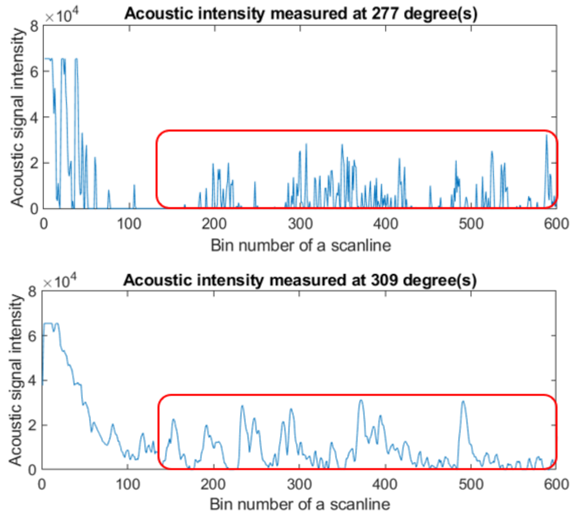

Figure 10. Plots showing different trends in multiple patches: a noisy plume (*top*) at a bearing angle of 277 ° and a relatively less noisy plume (*bottom*) at a bearing angle of 309 °, respectively.

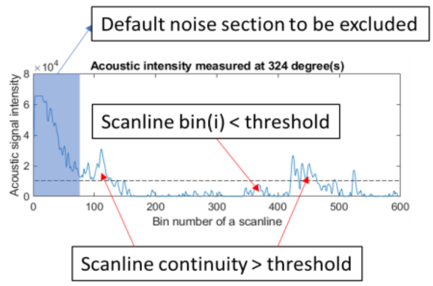

Figure 11. Measurement analysis in dimensional steps. The shaded box in blue indicates that the default noise section was excluded.

The in-situ measurements can be analysed in dimensional steps as shown in Fig. 11. **0-D Point data analysis:** Each intensity is stored as a numerical value in each bin; therefore, the lower intensity data below a fixed threshold can be ignored or excluded in the analysis. **1-D Line data analysis**: Continuity can be determined by counting the number of continuous positive (meaning those above the threshold) intensity data. By setting a certain number of counts above the threshold to be achieved for a signal to be recorded, false positives or negatives can be tolerated. These continuous peaks can be considered as a group (or a patch) that is differentiated from other patches. Combining the information of the distance between each group, the number of patches which lie across each straight scan line can be estimated. Three example cases with a threshold count of 5, are described in Table II. **2-D Plane data analysis**: The next step is to discern connectivity between scanlines to grasp a wider picture of a patch or a plume in the horizontal plane. The suggested steps of the analysis are shown in Fig. 12 which is a briefly summarised concept to establish the analysis direction.

TABLE II. THREE ANALYSIS CASES TO IDENTIFY PATCHES. THE TOTAL NUMBER OF PATCHES IS RESPECTIVELY CALCULATED WITH THE 1-D CONTINUITY CRITERIA

Case-I

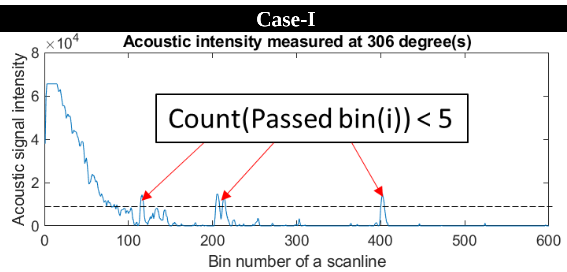

Patch quantity = 0

Description:

Peaks are detected at three locations; however, they were not considered as patches due to an insufficient number of continuous peaks.

Case-II

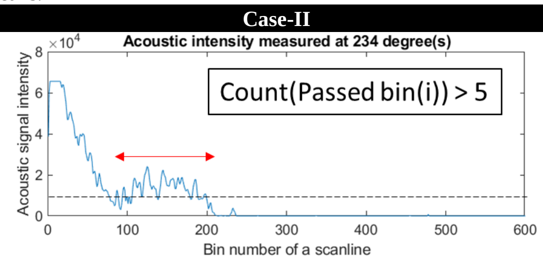

Patch quantity = 1

Description:

Continuous peaks of more than 5 were detected and this is categorised here as a patch.

Case-III

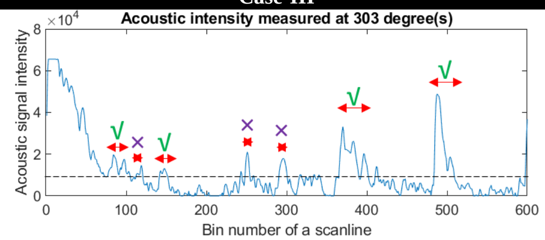

Patch quantity = 4

Description:

Numbers of peaks appeared at numerous locations. Only four groups of peaks met the continuity criteria, hence, there are four patches.

V. DISCUSSION

Due to the operating mechanism of the Ping360, a complete set of sonar measurements around the AUV is not instantaneously obtained. This means that an inevitable delay occurs in the data from the beginning to end of the scan of a sector during which time the AUV moves forward a certain distance. The influence of this delay can be minimized by reducing the scanning time or by increasing the complexity of the analysis (the latter also adds to the delay in obtaining a tracking result). The length of delayed time for a complete scan depends on the scanning range and scanning sector: Greater range and sector requires a longer scanning time. For example, with 50m range it takes 36 seconds for a 360˚ scan, while it can be reduced to 9 seconds when the range is decreased to 2m. The 36 seconds' wait is long enough for an AUV to pass or to lose track of a plume, whereas a 2m range is too short-sighted. Therefore, it is important to optimise the balance between a sufficient range and a limited delayed time. Similarly, it is also important to determine a minimum sector requirement for effective detection once the optimal range is decided. For example, a 360˚ scan (taking 16.3 seconds for a range of 15m) may not be necessary when the mission objective is to seek a plume ahead of the AUV. However, a too narrow scanning sector might not provide a meaningful sensing result. For our future reference, we created a guidance table displaying required time relative to range and sector based on empirical measurements. Fig. 13 shows a part of this guidance as an example.

Figure 12. The pseudo code for real-time analysis of in-situ acoustic intensity measurements.

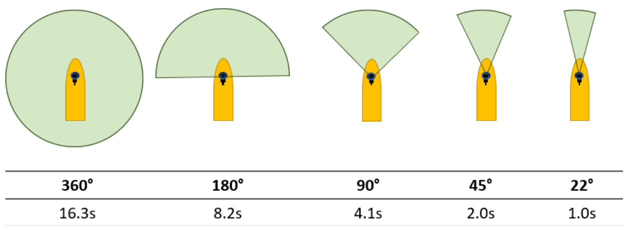

Figure 13. Required time for varied scanning sector at a 15m range.

By using a limited scanning sector looking forward from the AUV, we propose that a patchy oil plume might be tracked using this sonar detection and analysis approach to guide the AUV (See Fig. 14). During this plume following motion, the vehicle will alternate between two modes: Detect and Lost. Once the vehicle makes its first detection, it will turn to port while moving forward, until the plume is out of the scanning sector. Then the vehicle will turn in the opposite direction until the plume is re-captured inside the scan. Through taking turns of Detect mode and Lost mode, it can complete the profiling of a plume.

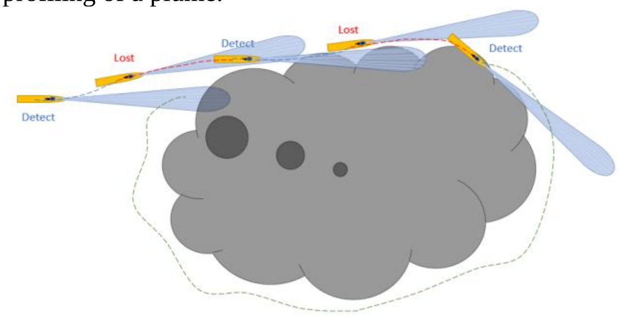

Figure 14. The proposed plume-following motion.

VI. Conclusion and Future Work

Petroleum leads to climate change through its combustion and the subsequent release of greenhouse gases, especially carbon dioxide. Although reducing petroleum use is the best long-term strategy to offset its effects on climate change, to date there have been limited research and incentives in place to promote viable, cost-effective alternatives to petroleum-based technologies. Petroleum pollutes the oceans directly through oil spills and indirectly through the release of petroleum-based products such as plastics and tyre particles. Oil spills jeopardise public health, pollute drinking water, destroy natural resources, and disrupt the economy. Effective oil spill response requires near real-time tracking of the movements of the oil in the ocean to minimise damage and reduce the time for environmental recovery.

In this paper, a sonar was proposed to be a substitute for more conventional oil detecting instruments. We present the performance of a Ping360 sonar that was evaluated in open water field tests with potential oil proxies in Lake Barrington, Australia. Relatively environmentally friendly targets were designed and tested during the field test and high visibility of the acoustic image of the proxies underwater remained throughout the field test. A crucial finding is that the collected real data included default noise, and this must be filtered before in-situ analysis during an AUV experiment.

One of the most significant merits of having a ‘scanning sonar’ integrated with the AUV is to allow a vehicle to continuously ‘see’ its updated surroundings while making zero contact with a target. By adopting a moving sensing instrument, a new survey design to surpass traditional gradient-following methods, that are only suitable for continuous plumes, can be devised; for example, an oil plume consisting of tens of small patches can be delineated by categorising and segregating out continuous signals with diverse layers of dimension.

In future work, our aim is to take these results and advance the capability of our designed algorithm to address survey of three-dimensional regions and to tackle the spatial-temporal issues that result in tracking a dynamic (moving) plume that is commonly the case in reality owing to currents. Our aim is to equip our AUV with true intelligence.

Conflict of Interest

The authors declare no conflict of interest.

Author Contributions

JH conducted the research and wrote the paper; NB supported and provided suggestions on the whole research paper; BR supported and assisted the oil release wave tank experiment; WT arranged the equipment and aided the project; the final results were discussed and approved by all members of the group of authors.

Acknowledgment

Funding was received from Fisheries and Oceans Canada through the Multi-Partner Oil Spill Research Initiative (MPRI) 1.03: Oil Spill Reconnaissance and Delineation through Robotic Autonomous Underwater Vehicle Technology in Open and Iced Waters and MPRI 1.15: Inshore Trials of Robotic Autonomous Underwater Vehicle Technology for Oil Spill Reconnaissance and Delineation using an Environmentally Friendly Proxy. This research was also supported by the Australian Research Council’s Special Research Initiative under the Antarctic Gateway Partnership (Project ID SR140300001), through an Australian Government Research Training Program Scholarship and a contract from Memorial University on Maritime Robotics to the first author. Further financial support came from the Natural Sciences and Engineering Research Council (NSERC) Discovery Grant programme to the second author: RGPIN-2021-02506 Advancing Autonomous Underwater Vehicle Capability for Assessment of Marine Pollution.

References

[1] B. Liddle and P. Sadorsky, "How much does increasing non-fossil fuels in electricity generation reduce carbon dioxide emissions?" *Applied Energy*, vol. 197, pp. 212-221, 2017.

[2] D. I. Little, S. R. Sheppard, and D. Hulme, "A perspective on oil spills: What we should have learned about global warming," *Ocean & Coastal Management*, vol. 202, p. 105509, 2021.

[3] D. S. Etkin and T. J. Nedwed, "Effectiveness of mechanical recovery for large offshore oil spills," *Marine Pollution Bulletin*, vol. 163, p. 111848, 2021.

[4] C. H. Peterson *et al.*, "Long-term ecosystem response to the Exxon Valdez oil spill," *Science*, vol. 302, no. 5653, pp. 2082-2086, 2003.

[5] U. H. Yim, M. Kim, S. Y. Ha, S. Kim, and W. J. Shim, "Oil spill environmental forensics: the Hebei Spirit oil spill case," ed: ACS Publications, 2012.

[6] C. Johannessen, P. Helm, B. Lashuk, V. Yargeau, and C. D. Metcalfe, "The tire wear compounds 6PPD-Quinone and 1, 3-Diphenylguanidine in an urban watershed," *Archives of Environmental Contamination and Toxicology*, pp. 1-9, 2021.

[7] R. N. Conmy *et al.*, "Dispersant effectiveness, in-situ droplet size distribution and numerical modeling to assess subsurface dispersant injection as a deepwater blowout oil spill response option and evaluation of oil fluorescence characteristics to improve forensic response tools," EPA/600/R-16/152, 2016. [Online]. Available: www.epa.gov/research

[8] E. Baszanowska and Z. Otremba, "Fluorometric index for sensing oil in the sea environment," *Sensors*, vol. 17, no. 6, p. 1276, 2017.
[9] R. N. Conmy *et al.*, "Submersible optical sensors exposed to chemically dispersed crude oil: Wave tank simulations for improved oil spill monitoring," *Environmental Science & Technology*, vol. 48, no. 3, pp. 1803-1810, 2014.
[10] J. Hwang, N. Bose, S. Fan, B. Robinson, and K. Tenekedjiev, "Complications of robotic delineation of oil spills at sea," in *Proc. the International Association of Maritime Universities (IAMU) Conference*, 2019, pp. 26-33.
[11] A. Balsley, K. Hansen, and M. Fitzpatrick, "Detection of oil within the water column," in *Proc. International Oil Spill Conference Proceedings*, American Petroleum Institute, vol. 2014, no. 1, 2014, pp. 2206-2217.
[12] T. Somekawa, J. Izawa, M. Fujita, J. Kawanaka, and H. Kuze, "Remote detection of oils in water using laser Raman spectroscopy," *Optics Communications*, vol. 480, p. 126508, 2021.
[13] D. McLeod, J. Jacobson, M. Hardy, and C. Embry, "Autonomous inspection using an underwater 3D LiDAR," in *Proc. 2013 OCEANS-San Diego*, 2013: IEEE, pp. 1-8.
[14] BlueRobotics. "Ping360 Scanning Imaging Sonar." [Online]. Available: https://bluerobotics.com/store/sensors-sonars-cameras/sonar/ping360-sonar-r1-rp/ (accessed June, 2021).
[15] A. Cihan and M. Y. Corapcioglu, "Effect of compressibility on the rise velocity of an air bubble in porous media," *Water Resources Research*, vol. 44, no. 4, 2008.

Jimin Hwang received the B.E. degree (Honours.) in Naval Architecture from the Australian Maritime College (AMC), University of Tasmania, Launceston, Australia, in 2016. Her thesis work focused on localization of autonomous underwater vehicles (AUVs) in a moving frame of reference. She is currently a Ph.D. candidate in maritime engineering at AMC and her project involves algorithm development of in-situ data-driven adaptive systems to control an AUV for tracking an oil plume. Her research interests include application of underwater robots for marine environmental problems, development of sensor-based reacting systems, and the design of artificial intelligence autonomous-decision making systems for marine robots.

Ms. Hwang was a recipient of the Tasmanian International Scholarship, Australian Government Research Training Program Scholarship and Antarctic Gateway Partnership Scholarship.

Neil Bose received the B.Sc. degree in naval architecture and ocean engineering from the University of Glasgow in 1978 and the Ph.D. degree from the University of Glasgow in 1982. He came to Memorial in May 1987 as an assistant professor in the naval architectural engineering program. He joined the Australian Maritime College (AMC) in 2007 as the Manager of the Australian Maritime Hydrodynamics Research Centre. He was also a Professor of maritime hydrodynamics with the AMC. From 2009 to 2011, he was the Director of the AMC's National Centre for Maritime Engineering and Hydrodynamics. He was Principal of AMC, University of Tasmania, from 2012-17. He was appointed as the Vice-President (Research) at the Memorial University of Newfoundland, Canada, in 2017. His research interests include marine propulsion, autonomous underwater vehicles, ocean environmental monitoring, ocean renewable energy and ice/propeller interaction.

Brian Robinson is Lab Manager with the Centre for Offshore Oil, Gas and Energy Research (COOGER) with Fisheries and Oceans Canada. He is located at the Bedford Institute of Oceanography in Dartmouth, Nova Scotia, Canada, with facilities including a mesoscale wave tank facility used for oil spill research. He has 15 years of experience in studying the fate and behaviour of crude oil in marine environments. His research areas of interest include analytical hydrocarbon analysis, oil droplet formation, and in-situ instrumentation used for oil spill monitoring.

Worakanok Thanyamanta received the B.Eng. degree in Environmental Engineering from Chulalongkorn University, Bangkok, Thailand, and the M.Eng. in Civil Engineering and the Ph.D. in Oil and Gas Engineering from Memorial University, St. John's, Canada. She has 12 years of experience in studying fluid dynamics and fluid-structure interactions, including experience working as a Computational Fluid Dynamics engineer at Oceanic Consulting Corporation and Fleetway, Inc.. She is now Research Associate and project manager of AUV projects as part of Fisheries and Oceans Canada's Multi-Partner Oil Spill Research Initiative. Her research interests include marine pollution, oil spill response, autonomous underwater vehicles, and ocean environmental monitoring.